Suppression of cell cycle progression by Jun dimerization protein (JDP2) involves down-regulation of cyclin A2

(Running title: cyclin A2 and JDP2 in cell cycle progression)

Jianzhi Pan[1, 2], Koji Nakade[1], Satoko Masuzaki[1], Hitomi Hasegawa[3], Yu-Chang Huang[4], Takehide Murata[1], Atsushi Yoshiki[1], Naoto Yamagichi[3], Yuichi Obata[1] and Kazunari K. Yokoyama[1, 4*]

[1]RIKEN BioResource Center, 3-1-1 Koyadai, Tsukuba, Ibaraki 305-0074, Japan; [2]Institute of Animal Husbandry and Veterinary, Zhejiang Academy of Agricultural Sciences, Hangzhou, Zhejiang, P. R. China; [3]Department of Molecular Cell Biology, Graduate School of Pharmaceutical Sciences, Chiba University, Chiba 260-8675, Japan; [4]Center of Excellence for Environmental Medicine, Graduate Institute of Medicine, Kaohsiung Medical University, 807 Kaohsiung, Taiwan.

*Correspondence and requests for materials should be addressed to Kazunari K. Yokoyama, Gene Engineering Division, BioResource Center, RIKEN, 3-1-1 Koyadai, Tsukuba, Ibaraki 305-0074, Japan (Tel: +81-29-836-3612; Fax: +81-29-836-9120; e-mail: kazu@kmu.edu.tw).

Abstract

We report here a novel role for Jun dimerization protein-2 (JDP2) as a regulator of the progression of normal cells through the cell cycle. To determine the role of JDP2 *in vivo*, we generated *Jdp2* knock-out (*Jdp2*KO) mice by targeting exon 1 to disrupt the site of initiation of transcription. The healing of wounded skin of *Jdp2*KO mice proceeded more rapidly than that of control mice and more proliferating cells were found at wound margins. Fibroblasts derived from embryos of *Jdp2*KO mice proliferated more rapidly and formed more colonies than wild-type fibroblasts. JDP2 was recruited to the promoter of the gene for

cyclin A2 (*ccna2*) at a previously unidentified AP-1 site. Cells lacking *Jdp2* had elevated levels of cyclin A2 mRNA. Moreover, reintroduction of JDP2 resulted in repression of transcription of *ccna2* and of cell cycle progression. Thus, transcription of the gene for cyclin A2 appears to be a direct target of JDP2 in the suppression of cell proliferation.

Key words: cyclin A2/*Jdp2* knock-out mice/cell proliferation/JDP2/skin wound healing/cell cycle arrest

The abbreviations used are: AP-1, activation protein-1; BrdU, bromodeoxyuridine; ChIP, chromatin immunoprecipitation; CRE, cAMP-responsive element; DRE, differentiation response element; EMSA, electrophoretic migration shift assay; GPDH, glycerol 3-phosphate dehydrogenase; JDP2, Jun dimerization protein 2; KO, knock out; MEF, mouse embryonic fibroblast; NE, nuclear extracts.

Introduction

Progression of the cell cycle in mammalian cells is regulated by the interplay of protein kinase complexes, known as cyclin-dependent kinases (CDKs), that are controlled by the levels of expression of their respective cyclin partners, which act as positive coactivators or as negative regulators in the case of the so-called cdk inhibitors (Grana and Reddy, 1995; Sherr and Roberts, 1999; Malumbress and Barbacid, 2009). While cyclin D-cdk4/cdk6 and cyclin E-cdk2 control progression through G_1 phase (Sherr, 1993) and cyclin B-cdc2 appear to be necessary for entry into mitosis (Furuno *et al*., 1999), cyclin A is a rate-limiting component required for both the initiation of DNA

synthesis and entry into mitosis (Pagano *et al*., 1992). There are two subtypes of cyclin A: cyclin A2, which is expressed almost ubiquitously, and cyclin A1, whose expression is restricted to the testis (Sweeney *et al*., 1996). In conditional cyclin A knock-out mice, the functions of cyclin A were essential for progression of hematopoietic cells and embryonic stem cells through the cell cycle but cyclin A is redundant in fibroblasts (Kalaszczynska *et al*., 2009). Expression of cyclin A is cell cycle-dependent with periodic relief of transcriptional repression.

Jun dimerization protein 2 (JDP2), a member of the AP-1 family, is able to form homodimers, and, also, heterodimers with other members of the AP-1 family, such as c-Jun, JunB, JunD and ATF2, and with a member of the C/EBP family, C/EBPγ (Aronheim *et al*., 1997; Jin *et al*., 2001; Broder *et al*., 1998). Assays involving ectopic expression of JDP2 indicated that JDP2 can block transformation of NIH3T3 cells and of lines of prostate cancer cells (Heinrich *et al*., 2004), whereas it also induces the partial transformation of chick embryonic fibroblasts (Blazek *et al*., 2003) and functions as a cell-survival protein in several cell lines (Lerdrup *et al*., 2005; Piu *et al*., 2001). JDP2 inhibits the differentiation of embryonal carcinoma F9 cells (Jin *et al*., 2002) and adipocytes (Nakade *et al*., 2007) and even promotes the differentiation of osteoclasts (Kawaida *et al*., 2003), C2 myoblasts and rhabdomyosarcoma cells (Ostrovsky *et al*., 2002). JDP2 is expressed ubiquitously and its level does not change significantly after diverse forms of cellular stimulations. In this regards, it seems to be quite distinct from other major AP-1 proteins, which are generally regulated by a variety of stresses at several levels, such as expression, stability, dimerization with other factors and DNA-binding activity.

JDP2 most likely participates in the repression of transcription via multiple mechanisms, which include DNA-binding competition and inactivation of formation of heterodimer with other members of the AP-1 (Aronheim *et al*., 1997), recruitment of HDAC 3 (Jin *et al*., 2002), inhibition of histone acetylation and the direct regulation of chromatin assembly (Jin *et al*., 2006). However, the details of the physiological role of JDP2 in cell fate remain unknown, and the mechanisms by which JDP2 acts as a regulator of the proliferation or transformation of cells remain to be clarified. Recently, we generated *Jdp2*-deficient mice, with a deletion in the promoter and non-coding exon 1 region of the *Jdp2* locus (*Jdp2*KO mice) and reported that "knock-out" of *Jdp2* affects adipocyte differentiation (Nakade *et al*., 2007) and resistance to replicative senescence (Nakade *et al*., 2009).

Although our *Jdp2*KO mice did not exhibit any apparent abnormalities under standard breeding conditions, we report here that loss of JDP2 results in accelerated cell cycling by embryonic fibroblasts (MEFs) and enhances the expression of cyclin A2 through loss of direct binding to the promoter of the gene for cyclin A at a previously unidentified AP-1 motif. We also observed that the accelerated cell growth in the healing of skin wounds in adult *Jdp2*KO mice. Our data indicate that the gene for cyclin A is a direct transcriptional target of JDP2 in the repression of cell proliferation by JDP2.

Materials and methods

Plasmid construction, electophoretic mobility shift assays (EMSA), immunopreciptation and IP-Western blotting (see in the supplementary methods)

Cell culture

Mouse embryonic fibroblasts (MEFs) were prepared from embryos at embryonic day 12.5 (E12.5) with a mixed genetic background of B6 and 129 as described elsewhere (Nakade *et al*., 2007). For serum-starvation experiments, MEFs were incubated in DMEM that contained 0.1% FCS for 48 h, at confluence; then they were re-plated in DMEM that contained 15% FCS.

Skin wound-healing model and scratch-wounding assay *in vitro*

*Jdp2*KO male mice at 20-30 weeks of age (body weight, 30.3 ± 0.7 g) were used in skin wound-healing assays, together with sex- and age-matched WT littermates (body weight, 29.5 ± 2.40 g). After shaving the dorsal hair and cleaning the exposed skin with 70% ethanol, we made full-thickness excision skin wounds aseptically unit a 4-mm biopsy punch. Each wound region was photographed digitally with a scale marker 1, 3, 6 and 9-11 days after wounding. The size of the unclosed wound bed was calculated with the Image J program (version 1.36b; NIH, USA). Wounded mice were injected intraperitoneally with 20 μl/g body weight of bromodeoxyuridine (BrdU) labeling reagent (Roche Applied Science, Penzberg, Germany) on various days after wounding and killed 2.5 h after injection. Paraffin-embedded sections were subjected to hematoxylin-eosin staining and immunostaining with the BrdU Labeling and Detection Kit I (Roche Applied Science). The endothelial cells and fibroblasts that had incorporated BrdU at wound margins were photographed under a fluorescence microscope with a digital camera system (Olympus, Tokyo, Japan). The scratch-wounding assay *in vitro* was performed with MEFs to mimic wound healing in individual mice. Confluent monolayer of cells were then scratched linearly and incubated for a few days in DMEM plus 15% FCS. Photographs were taken 12 to 60 h after scratching.

Analysis of cell proliferation and the cell cycle

MEFs were cultured at 5 x 10^5 cells per 10-cm dish or 2 x 10^4 cells per well in 24-well plates, in triplicate, to estimate proliferation rates. Cells were counted by the trypan blue dye-exclusion test (Gibco-Invitrogen) or after application of the Alamar Blue reagent (Alamar Biosciences, Sacramento, CA, USA) according to the manufacturers' instructions. For analysis of the cell cycle, serum-starved MEFs were further cultured in DMEM that contained 15% FCS and collected at the indicated times. Harvested cells were stained with propidium iodide (PI; 1 μg/ml), and subjected to fluorescence-activated analysis of DNA content in a flow cytometer EPICS XL-MCL; Beckman Coulter, Miami, FL, USA). Percentages of cells at each phase of the cell cycle were determined. To count cells that had entered the S-phase from the G_1-or G_0-phase at higher sensitivity, we performed a BrdU-incorporation assay *in vitro* with the BrdU Labeling and Detection Kit I. Serum-starved MEF were seeded at 1 x 10^5 cells per chamber on chamber slides in DMEM plus 15% FCS. After 12 h, cells were pulse-labeled for 3 h with 10 μM BrdU and the BrdU incorporated into cells was detected by immunocytochemical staining with antibodies against BrdU and fluoresceine-conjugated second antibodies, together with staining with PI for localization of nuclei. For the colony-formation assay, MEFs were plated in duplicate at 5 x 10^2 or 5 x 10^3 cells per 10-cm gelatin-coated dish. After two weeks, colonies with diameters greater than 2 mm were counted after staining with Giemsa staining solution (Wako Chemicals, Co., Tokyo, Japan).

Isolation of RNA, microarrays and real-time quantitative RT-PCR

Total RNA was extracted from various tissues of both *Jdp2*KO and WT adult mice, from embryos and from corresponding MEFs with Trizol (Invitrogen) according to the

manufacturer's instructions. Expression of JDP2 mRNA was analyzed by Northern blotting as described elsewhere (Jin *et al*., 2002). For microarray analysis, total RNA (5 μg) was converted to cRNA with aminoallyl-UTP and fluorescence-labeled with a low-input RNA linear amplification kit (Agilent Technologies, Inc., Santa Clara, CA USA) and Cy3- or Cy5-labeled CTP (PerkinElmer, Waltham, MA, USA). Samples of Cy3-labeled WT RNA and Cy5-labeled JDP2-deficient RNA (750 ng) were combined in equal amounts and allows to hybridize to a microarray (Agilent Mouse Oligonucleotide Array, 22,000 features, Agilent Technologies Inc.) for 17 h at 60 °C, with subsequent washing, drying and storage under nitrogen in darkness. Hybridization signals recorded with a microarray scanner (Agilent) were normalized and corrected for background signals (with Agilent Feature-Extraction software). Real-time quantitative RT-PCR (qRT-PCR) was performed with a PRISM™ 7700 system (Amersham Biosystems Instruments, Foster City, CA, USA) according to the manufacturer's instructions. We designed the primers using the public-domain Primer 3 program of GENETYX-Mac Ver.14 software (Hitachi Software, Tokyo, Japan). The respective pairs of primers were listed in Supplementary Table 2.

Promoter reporter assays

Cyclin A2 promoter-reporter DNAs were transfected into WT and *Jdp2*KO MEFs with or without pcDNA3-JDP2 or pcDNA3 empty vector at 1 μg of total DNA per well of a 24-well plate (5×10^4 cells/well) using 2 μl of Lipofectamine^{TM}-2000 reagent (Invitrogen). A series of JDP2 promoter-reporters were transfected in a similar way as described elsewhere (Jin *et al*., 2002; Nakade *et al*., 2006).

Assay of cyclin A2-associated kinase activity

We immunoprecipitated total cellular proteins with antibodies against cyclin A2 and protein A-Sepharose beads. The beads with bound immune complexes were mixed with [^{32}P]-ATP and histone H1 peptide substrate (cat. no. 14-155; Upstate biotechnology Co.) in a kinase assay buffer [50 mM HEPES (pH 7.0), 10 mM $MgCl_2$, and 1 mM dithiothreitol) for 30 min at 30 °C. Reaction products were resolved by SDS-PAGE (12% polyacrylamide) and phosphorylated histone H1 peptide was detected by autoradiography.

Adenoviral infection

Replication-defective adenovirus that encoded JDP2 (Ad-JDP2) and β-galactosidase (Ad-cont) were generated from pAxCAwt, as described elsewhere (RIKEN DNA Bank; Miyake *et al*., 1996, Ugai *et al*., 2005).

siRNA transfection

4 x 10^4 WT and *Jdp2*KO MEFs at 60% confluence were transfected with 20 pmole of control siRNA (Invitrogen 45-2002; lot 360646) and two siRNAs (#1 and #2; Nakade *et al*., 2009) against JDP2 according to the manufacturer's instruction (Amgene and Invitorgen, respectively).

Analysis of data

Results are expressed as the mean plus or minus the standard deviation (± SD) of results for each set of replicates. Statistical comparison of single parameters between two groups was performed by a paired Student t-test. P values of less than 0.05 or 0.01 were considered significant.

Results

Assays of skin-wound healing and scratch wounding

To investigate the functional impact of loss of expression of the *Jdp2 in vivo*, we used a model of skin-wound healing to compare the healing of skin between WT and *Jdp2*KO mice. Male C57/BL6J mice were injured by excising full-thickness skin (a disk of 4 mm in diameter) from their shaved backs. In control WT mice, re-epithelialization was complete within 11 to 13 days after injury. In the case of *Jdp2*KO mice, the skin seemed to re-epithelialize rapidly within 10 to 11 days. Recovery of skin wounds was examined by macroscopic observation of the wounded skin on days 1, 3, 6 and 10 after injury (Figure 1A). We measured the area of the wound in each case and found that wound repair was accelerated in *Jdp2*KO mice (Figure 1B). In order to compare the proliferative potential of cells after tissue injury in *Jdp2*KO and WT mice, we labeled wound mice with bromodeoxyuridine (BrdU) *in vivo*. Wounded mice were injected intraperitoneally with BrdU at 0, 1, 3 and 6 days after wounding and sacrificed 2.5 h after injection. Samples of skin wounds were excised for the preparation of paraffin-embedded sections, which were subjected to immunostaining with antibodies against BrdU (Figure 1C). We found large numbers of BrdU-positive endothelial cells and fibroblasts at wound margins, and the numbers of BrdU-positive cells at wound margins in *Jdp2*KO mice were 2- to 5-fold higher than in WT mice. Thus, enhancement of cell proliferation in *Jdp2*KO mice apparently contributed to enhanced repair of wounds. Levels of mRNAs for PCNA, Col1a1 and cyclin A2 were higher in the skin of *Jdp2*KO mice than in that of WT mice 1, 3 and 6 days after injury (Figure 1D). Thus, JDP2 was clearly involved in the expression of growth-related genes, such as those for PCNA, Col1a1 and cyclin A2.

We performed wound-scratch assays *in vitro* with mouse embryonic fibroblasts (MEFs) that mimic the phenomenon of wound healing in intact mice. The rate of

migration into the scratch of *Jdp2*KO MEFs was 1.4-fold higher than that of WT MEF (Figure 1E). At 36 h, the wounded area had disappeared in the case of MEFs from *Jdp2*KO mice but not from WT MEFs (data not shown). The rate of migration into the scratch of *Jdp2*KO MEFs was 1.4-fold higher than that of WT MEF. These data indicate that the JDP2 is involved in the suppression of cell proliferation in WT MEF.

Control of the proliferation of *Jdp2*-deficient cells

We prepared MEFs from *Jdp2*KO embryos on day 12.5 post coitus. Northern blotting analysis both of embryos and of isolated MEFs failed to reveal any JDP2 mRNA when we used a DNA probe from the *Jdp2* coding region (Figure 2A) and when we used a DNA probe that corresponded to the 3' non-coding region (data not shown). Thus, expression of JDP2 mRNA had been completely disrupted in embryos and MEFs from *Jdp2*KO mice. Controls from WT embryos yielded the expected size of JDP2 mRNA.

We next performed Western blotting analysis of lysates of MEFs from WT and *Jdp2*KO mice using antibodies against JDP2 (a gift from Dr. A. Aronheim; Figure 2B). Bands specific for JDP2 (18.5 kDa) were detected in the analysis of WT MEFs but not in that of *Jdp2*KO MEFs in both assays with the different JDP2-specific antibodies.

In our analysis of cell proliferation, we examined the proliferation of MEF using three different assays, namely, trypan blue dye-exclusion, the Alamar Blue assay, and colony formation. Figure 2C shows that *Jdp2*KO MEFs proliferated more rapidly than WT MEFs when plated at 5×10^5 cells per 10-cm dish in DMEM plus 10% FCS. The results of the cell growth assay with Alamar Blue dye also supported this conclusion (Figure 2D). The colony-formation assay also confirmed this result. We plated 5×10^2 cells and 5×10^3 cells in gelatin-coated 10-cm dishes and counted colonies (of more than 2 mm in diameter) after two weeks. The *Jdp2*KO MEFs were able to form colonies

more efficiently than the WT MEFs (Figure 2E). These results indicated that JDP2 plays a critical role in growth control both *in vitro* and *in vivo*.

Absence of a requirement for JDP2 in apoptosis induced by UV and DNA-damaging reagents

Piu *et al*. (2001) reported that JDP2 plays a critical role in UV-induced apoptosis. However, evidence for such a role was only provided by results of experiments that involved over-expression of JDP2 in specific cell lines. We found that UV-irradiated MEFs underwent apoptosis in a dose- dependent manner at doses of UVC from 20 to 60 J/m^2, but we did not detect any obvious difference between WT and *Jdp2*KO MEFs in subsequent trypan blue dye-exclusion assays (Supplementary Figure 3A) and assays of the activities of caspases 3 and 7 (Supplementary Figure 3B). When MEFs were exposed to UVC at 60 and 600 J/m^2, for 2 h and 8 h, the level of expression of JDP2 fell significantly (Supplementary Figure 3D). We also irradiated MEFs with UVC at 20 J/m^2, incubated them for another 24 h, and then subjected them to flow cytometry to assess levels of sub-G_1 cells. The size of the sub-G_1 population of UV-irradiated MEFs from *Jdp2*KO mice was identical to that of MEFs from WT mice (Supplementary data 3C). We also examined the effects of a set of chemical inducers of apoptosis. We exposed MEF to various inducers of apoptosis, such as actinomycin D (10 μM), camptothecin (2 μM), cycloheximide (100 μM), dexamethasone (100 μM), and etoposide (100 μM) for 24 h. All reagents induced increases in the activities of caspases 3 and 7 in a dose-dependent manner (data not shown), but no significant differences in respective activities were found between WT and *Jdp2*KO MEFs (Supplementary Figure 4) except after the application of cycloheximide, an inhibitor of protein

synthesis. These data suggested that JDP2 has no significant effect on the apoptotic responses to UV and inducers of cell death in normal MEFs.

We next performed a cell cycle re-entry assay, counting propidium iodide-stained (PI-stained) MEFs by flow cytometry. MEFs cultured in serum-free medium were re-stimulated by addition of 15% FCS and then harvested at various time after the addition of FCS. One representative experiment showed that 28% of *Jdp2*KO MEFs were in the S-phase, while only 20% of WT MEFs were in the S-phase after 18 h of stimulation (Figure 3A). The number of MEFs derived from *Jdp2*KO mice in the S-phase was considerably higher than that of WT MEFs (Figure 3B). Proliferation of *Jdp2*KO MEFs was accelerated as a result of enhanced progression of cells from the G_1- or the G_0-phase to the S-phase, and not as a result of differential activity related to cell death.

We also examined the incorporation of BrdU into MEFs. Serum-starved MEFs were seeded in chamber slides at a given density in DMEM plus 15% FCS. After incubation for 12 h, cells were pulse-labeled with 10 μM BrdU for 3 h. Cells in S-phase that had incorporated BrdU were detected with antibodies against BrdU and fluorescein-conjugated second antibodies (Figure 3C). The percentages of BrdU-positive cells in six areas of chambers demonstrated that *Jdp2*KO MEFs moved more frequently from a quiescent state to a proliferative state than did WT MEFs (Figure 3D).

Regulation of cell cycle-related genes by JDP2

To examine the role of JDP2 in the cell cycle, we analyzed the expression of individual cell cycle-related genes. MEFs were arrested at the G_0/G_1-phase by deprivation of serum for 48 h, and then re-entry into cell cycle was triggered by re-plating in DMEM plus 15% FCS. As shown in Figure 4A, no notable differences in levels of proteins, such as cyclin D1, cyclin D3, cdk4, cdk6 and Rb were detected between WT and

*Jdp2*KO MEFs. Levels of p53 and p21 in *Jdp2*KO MEFs were lower than those in WT MEFs after induction by serum (Figure 4A).

We next examined global gene expression in *Jdp2*KO MEFs using an oligo DNA microarray from Agilent Technologies, Inc. (Santa Clara, CA, USA), known as "Mouse". We extracted total RNA from WT MEFs and from *Jdp2*KO MEFs, which had been synchronized by serum-starvation for 48 h and then stimulated with 15% FCS in DMEM for 14 h. The genes identified included up- or down-regulated genes, genes for cyclins and p53-related genes, as listed in Figure 4C and the entire data set from the microarray analysis is available at the CIBEX database (CIBEX, Mishima, Japan; CIBEX accession, CBX101). Elevated expression of genes for cyclin A2 and cyclin E2 was detected in *Jdp2*KO MEFs as compared to WT MEFs. Conversely, genes for the cyclin-dependent kinase inhibitor p21, p16 and p15, but not for p27, were expressed at lower levels in *Jdp2*KO MEFs than in WT MEFs. Genes from families of apoptosis-related genes and genes for other AP-1 and C/EBPs did not reveal any remarkable differences between *Jdp2*KO and WT MEFs, exception in the case of JDP2 and C/EBPδ. Expression of 21 known genes differences between Jdp2KO and WT MEF, was enhanced and that of 20 known genes was depressed in *Jdp2*KO MEFs (Supplementary Table 1).

We performed two microarray assays and each assay revealed the increased expression of genes for cyclin A2 and cyclin E2 and the decreased expression of genes for p21, p16 and p15 in *Jdp2*KO MEFs. Moreover, as shown in Figure 4B, the correlation coefficient with respect to the relative changes in levels of mRNAs between the two assays was higher than 0.8, indicating that the data from the microarrays were valid.

We compared the levels of expression of mRNAs in WT MEFs and *Jdp2*KO MEFs by real time RT-PCR, respectively, before and after re-stimulation with serum. We examined the levels of the transcripts of representative genes, which appeared to have risen or fallen in microarray studies, as well as those of members of the AP-1/ATF family, including c-Jun, c-Fos and JunD. The results were consistent with those in the microarray assay (Figures 4C and 4D).

Cyclin A2 is a target of JDP2

Our microarray study indicated that JDP2 might be involved in the negative regulation of progression of the cell cycle via regulation of the expression of the gene for cyclin A2 (*ccna2*). We examined the level of cyclin A2 mRNA by real-time PCR after re-stimulation of MEF by serum. The expression of cyclin A2 was enhanced by addition of FCS in both lines of MEFs. However, a more significant increase (1.5- to 2.0-fold) in the expression of cyclin A2 was noted in *Jdp2*KO MEFs than in WT MEFs after stimulation. In parallel, we also measured the kinetics of changes in levels of mRNA for JDP2 and c-fos (Figure 5A). The expression of JDP2 mRNA decreased slightly after serum stimulation in WT MEF. By contrast, expression of c-fos mRNA rose rapidly but transiently within 4 h after the start of stimulation, without any significant difference between the two lines of MEFs. As shown in Figure 5B, levels of mRNAs for cyclin A2 and cyclin E2 were significantly higher and expressions of both genes started earlier in *Jdp2*KO MEFs than in WT MEFs after the re-addition of serum. By contrast, expression of the cell cycle inhibitor $p16^{Ink4a}$ decreased gradually for the first 6 h after the start of stimulation with FCS only in *Jdp2*KO MEFs. The expression of p21 mRNA remained almost unchanged in both lines of MEFs.

We performed a chromatin immunoprecipitation (ChIP) assay to investigate whether or not JDP2 regulates the expression of its target genes directly. Immunoprecipitated proteins with monoclonal antibodies against JDP2 (#176) were applied to PCR for detection of promoter target regions of genes for cyclin A2, cyclin E2, and $p16^{Ink4a}$, respectively. We detected products of PCR that corresponded to the promoter regions of genes for cyclin A2 and $p16^{Ink4a}$ in the sonicated chromatin derived from WT MEFs but not from *Jdp2*KO MEFs (Figure 5C). In the case of cyclin E2, no specific band was detected and only faint bands appeared after amplification for 45 cycles, even when we used JDP2- deficient cells. Our data indicated that genes for cyclin A2 and $p16^{Ink4a}$ are the most likely targets of JDP2 in progression of the cell cycle, even though they exhibited opposite responses upon serum stimulation of serum-starved cells. After the addition of FCS, JDP2 appeared to be recruited to the transcriptional regulatory region of the gene for cyclin A2 and to be released from the $p16^{Ink4a}$ locus.

Promoter analysis of the gene for cyclin A2

We cloned a 1,101-bp fragment of DNA from the 5' region of the mouse gene for cyclin A2 and constructed a series of promoter deletion-luciferase genes (Figure 6A). We deteted 2.5- to 4.5-fold higher luciferase activity in *Jdp2*KO MEFs than in WT MEFs when we tested this series of deletion constructs, even though the activities due to the control reporter vector, with an SV40 promoter, were identical in both lines of MEFs (Figures 6B and 6D). Moreover, deletion of the *Sac*I-*Xho*I fragment that contained the AP-1 site increased luciferase activity in WT MEFs but not in *Jdp2*KO MEFs, suggesting that the region from *Sac*I to *Xho*I is important for JDP2-mediated repression of the expression of cyclin A2. A point mutation at the AP-1 site enhanced luciferase

activity in WT MEFs but not in *Jdp2*KO MEFs (Figure 6C). By contrast, a point mutation at the CRE or at both the AP-1 site and the CRE resulted in decreased luciferase activities in both lines of MEFs, indicating that the CRE has *cis*-activity in the cyclin A2 promoter that is under the control of CRE-binding activators, even though JDP2 might still be a repressive component in the activation complex. When we transfected cells with reporter constructs p3AP1 and p3CRE, in which a 3x AP-1 consensus sequence or a 3x CRE consensus sequence had been inserted in the TK-luciferase vector (Promega), the luciferase activities due to these constructs were higher in *Jdp2*KO MEFs than in WT MEFs (data not shown), supporting the definition of JDP2 as an AP-1/CRE-dependent repressor in MEF (Aronheim *et al*., 1997; Jin *et al*., 2002).

To determine whether JDP2 represses the expression of the gene for cyclin A by exploiting its histone-modification activity, as described previously (Jin *et al*., 2006), we performed ChIP assays with antibodies against acetyl-H4 to assess the histone-acetylation status of the promoter region of the gene for cyclin A in WT and *Jdp2*KO MEFs. The level of actylation of histone H4 in *Jdp2*KO MEFs was clearly higher than that in WT MEFs (Supplementary Figure 5).

Binding of JDP2 to the cyclin A2 promoter

We performed electrophoretic mobility shift assays (EMSAs) to verify the DNA-binding activity of JDP2 using oligodeoxynucleotide probes that corresponded to the AP-1 site, the CRE and the AP-1-like site, as a control. As shown in Figure 7A, the AP-1 and CRE probes but not the AP-1-like probe generated large DNA-protein complexes with nuclear extracts from either WT MEFs or *Jdp2*KO MEFs (lanes 2 and 3 for CRE; and lanes 8, 9 and 11 for AP-1). The corresponding unlabeled competitors released

[^{32}P]-radiolabeled-oligodeoxynucleotides from the DNA-protein complexes (compare lanes 13 to 15 with lane 11), but less effective competition was observed with an AP-1 mutant oligodeoxynucleotide (lane 12). When we added antibodies specific for JDP2 (#249) to the reaction mixture with the AP-1 probe, we detected super-shifted bands in the case of nuclear extracts from WT MEFs but not from *Jdp2*KO MEFs (compare lane 2 with lane 4 and lane 6 with lane 8 in Figure 7B). Moreover, the band in the case of serum-stimulated WT MEFs was less intense than that from serum-starved WT MEFs, indicating that addition of FCS suppressed the formation of a protein-DNA complex that included JDP2 under these conditions. By contrast, the CRE oligodoxynucleotide-protein complex was shifted by addition of antibodies specific for JunD but not by antibodies specific for JDP2 (Figure 7C), indicating that the CRE site "preferred" members of the AP-1 family other than JDP2. These data strongly suggest that JDP2 binds to the AP-1 site of the promoter of the gene for cyclin A2 and the induction of progression of the cell cycle with serum suppressed formation of the JDP2-DNA complex.

Elevated levels of the cyclin A2/cdk2 complex and of cdk activity in *Jdp2*KO cells

We detected cyclin A2 by Western blotting of lysates of MEFs prepared at various time after re-stimulation with FCS. The level of cyclin A2 was 3-to 5-fold higher in *Jdp2*KO MEFs than in WT MEFs, irrespective of whether the source of extracts was whole cells or nuclei (Figure 8A). We immunoprecipitated cdk2 with antibodies against cdk2 from equal amounts (as 400 μg protein) of cell lysate prepared from WT and *Jdp2*KO MEFs 0, 8, 16 and 20 h after re-addition of FCS. Immunoblotting with antibodies specific for cyclin A and cdk2, and for β-actin as a control, revealed that the amount of cyclin A associated with cdk2 was dramatically increased by serum stimulation, even though the

level of cdk2 was almost constant. Moreover, the level of the cyclin A/cdk2 complex in *Jdp2*KO MEFs was 2-to 3-fold higher than in WT MEFs, with the difference being especially marked 16 to 20 h after the re-addition of FCS (Figure 8B)

In an attempt to measure levels of cyclin A2-associated kinases, such as cdk2, we prepared lysates from WT and *Jdp2*KO MEFs and subjected them to immunoprecipitation with antibodies against cyclin A2. Then we mixed immune complexes with [γ ^{32}P]-ATP and histone H1 peptide as a substrate in a kinase assay buffer. The resultant phosphorylated H1 peptide was detected by SDS-PAGE and autoradiography (Figure 8C). We found that lysates from *Jdp2*KO MEFs had several-fold-higher kinase activity than those from WT MEFs (based on the radioactivity).

Repression by JDP2 of cell growth and the reporter activity of the cyclin A2 promoter

We examined the effects of JDP2 on the proliferation of MEF by over-expressing JDP2 in WT MEFs and re-expressing JDP2 in *Jdp2*KO MEFs. First, we introduced a JDP2 expression vector into WT and *Jdp2*KO MEFs and we monitored cell numbers with Alamar Blue three days after transfection (2- to 3-fold increase of JDP2 mRNA expression; data not shown). As shown in Figure 9A, the JDP2 expression vector suppressed cell growth in both lines of MEFs, and the effects in *Jdp2*KO MEFs were more significant than in WT MEFs.

We used the cyclin A2 promoter-reporter construct pA2M and the corresponding construct with a mutation at the AP-1 site to examine the effect of re-expression of JDP2 in *Jdp2*KO MEFs. Transfection with pcDNA-JDP2 reduced the reporter luciferase activity significantly in the case of pA2M, but not in the case of the mutant reporter

pA2mAP1 (Figure 9B). These data suggested, yet again, that JDP2 represses the activity of the cyclin A2 promoter, in a manner dependent specifically on the AP-1 site.

When we used a recombinant adenovirus vector that encoded JDP2 to induce its over-expression, infection with the JDP2-expressing virus significantly suppressed cell growth in both WT and *Jdp2*KO MEFs, acting in a dose-dependent manner, even at an m.o.i. of 1 (Ad JDP2 increases 50- to100-fold expression of JDP2, Nakade *et al*., 2009). The expressed JDP2 almost halved the number of WT and *Jdp2*KO MEFs on day 5 (Figure 9C). Moreover, expression of cyclin A2 was significantly depressed in both lines of MEFs (Figure 9D). Thus, ectopic expression of JDP2 appeared to suppress the proliferation of MEFs by regulating the expression of cyclin A2.

We also examined the effects of JDP2-specific siRNAs on the proliferation of MEFs. In WT MEFs, two different JDP2-siRNA constructs reduced the expression level of JDP2 by as much as 50% (Figure 9F). These siRNAs accelerated the proliferation of WT MEFs but not of *Jdp2*KO MEFs (Figure 9E). Moreover treatment with JDP2-siRNA of WT MEFs increased the level of cyclin A2 mRNA but reduced the level of cyclin A2 mRNA in *Jdp2*KO MEFs (Figure 9F). These data strongly suggest that JDP2 represses progression of the cell cycle via the expression of cyclin A2, thereby inhibiting the proliferation of mouse MEFs.

Discussion

In the present study we demonstrated that loss of JDP2 allows the enhanced expression of cyclin A2, which stimulates the proliferation of mouse skin and embryonic fibroblasts (MEFs). Wounds in the skin of *Jdp2*KO mice healed more rapidly than those in the skin of WT mice (Figures 1A and 1B), with larger numbers of proliferating

cells at the wound margins in *Jdp2*KO mice (Figure 1C). Incorporation *in vivo* of BrdU into DNA in skin from *Jdp2*KO mice was more than 1.8-fold higher than that in skin from WT mice. The scratch-wounding assay of MEFs *in vitro* also showed the same conclusion (Figure 1E). These activities are indicated as the proliferation capacity of cells. The cell proliferative activity of *Jdp2*KO MEFs was much higher than that of WT MEFs (Figure 2D), no matter what the number of passages (Figure 2C), as was the rate of formation of foci (Figure 2E). Moreover, more cells had entered S-phase in cultures of *Jdp2*KO MEFs than in those of WT MEFs 18 h after serum induction (28% vs 20% in Figure 3A) and approximately 3.7-fold more of BrdU-incorporating cells were detected (Figure 3C). Taken together, these different assays revealed the elevated proliferative potential of MEFs from *Jdp2*KO, as compared to WT MEFs and furthermore, JDP2 does not affect apoptosis but controls proliferation, at least in normal cells (Supplementary Figure 3).

To identify the target gene of JDP2, we used a mouse microarray to identify changes in levels of transcripts of genes related to the cell cycle, of genes for some growth factors and of genes for some AP-1/ATF transcription factors in *Jdp*2KO MEFs. After serum induction, the level of cyclin A2 mRNA rose 2- to 3-fold in *Jdp2*KO MEF, as compared with that of WT MEFs (Figures 5A and 5B). We examined the promoter of the gene for cyclin A2 in terms of DNA-binding proteins and specific binding sites. The effects of mutation of the AP-1 site were clear in WT MEFs but not in *Jdp2*KO MEFs. By contrast, mutation of the CRE resulted in lower activity in both line of MEFs (Figure 6C). A gel shift assay demonstrated that no proteins bound to the far-upstream AP-1-like site, while the AP-1 site and CRE recruited specific proteins to form DNA-protein complexes (Figure 7A). In the case of the AP-1 site, JDP2 was included in the

shifted DNA-protein complex, but no shifted band was detected in the case of nuclear extracts of *Jdp2*KO MEFs. When WT MEFs were stimulated with serum, the intensity of the shifted band that included JDP2 decreased significantly (compare lanes 2 and 6 in Figure 7B). In the case of cyclin E2, the level of mRNA fell transiently from 3 to 8 h after addition of serum and then gradually returned to its initial level (Figure 5B). However, no AP-1/CRE elements have been found in the promoter region of the gene for cyclin E2. Thus, regulation of transcription of cyclin E2 might be other mechanism like histone modification (Jin *et al*, 2006; nakade *et al*, 2009) or translational regulation of cyclin E2 (Mullany *et al*, 2007).

Previous studies demonstrated that JunB binds to the CRE at S-phase (Andrecht *et al*., 2002). ChIP assays also demonstrated that JunB binds to this CRE in ras-transformed rat thyroid cells in G_2 (Casaline *et al*., 2007), as confirmed subsequently in exponentially growing HeLa cells (Farras *et al*., 2008). Farras *et al*. (2008) also demonstrated that the AP-1 site can bind JunB- and Fra-1-containing AP-1 dimers more efficiently than the CRE. In ras-transformed cells, levels of both Fra-1 and JunB are dramatically higher than in the normal cell counterparts (Casalino *et al*., 2003; Piechaczyk and Farras, 2008). However, in our present study, we found that JunD and c-Fos, and not JunB and Fra-1, bound to the CRE in mouse WT MEFs. Thus, the composition of the AP-1 complex might differ among cell types, playing a critical role in the expression of cyclin A2 to promote progression of the cell cycle. We found that JDP2 is recruited only to the AP-1 site of the cyclin A2 promoter for negative regulation of transcription.

It remains to be determined whether the AP-1 site is functional or not. The present study demonstrated, first, that the AP-1 site is critical for the repression of the cyclin A2

promoter by JDP2. We also demonstrated that cyclcin A2 associates with cdk2 to exhibit cdk-kinase activity (Figure 8). The expression of cyclin A2 is elevated in *Jdp*2-null cells and then cdk-kinase activity is enhanced, with promotion of cell proliferation.

JunB-Expressing fibroblasts exhibit proliferative defects that are due to an extended G_1-phase. The accumulation of JunB leads to cell-cycle arrest in G_1 via induction of the expression of the gene for an inhibitor of a cell-cycle-related kinase, $p16^{Ink4a}$ (Passegue and Wagner, 2000). Moreover, overexpression of JunB antagonizes c-Jun-mediated induction of the expression of cyclin D1 in G_2 (Bakiri *et al*., 2000). Cells are, consequently, blocked before they can enter S-phase, with possible subsequent senescence (Passegue and Wagner, 2000). The proposed anti-proliferative function of JunB is supported by the observation that JunB-null transgenic mice with a myeloproliferative disease progress to "blast crisis" (Passegue *et al*., 2001). The absence of JunB expression results in down-regulation of the expression of $p16^{Ink4a}$ and elevated levels of c-Jun (Passegue *et al*., 2001).

In a similar way, we reported recently the down-regulation of $p16^{Ink4a}$ on *Jdp2*MEFs through the binding of JDP2 to histone (Nakade *et al*., 2009). In the present study, the level of $p16^{Ink4a}$ mRNA was reduced from 6 to 16 h after the start of serum induction, recovering again at 20 h (Figure 5B). The level of $p16^{Ink4a}$ was significantly lower in *Jdp2*KO MEFs than in WT MEFs, so we examined the recruitment of JDP2 to the promoter regions of genes for cyclin A2 and $p16^{Ink4a}$ (Nakade *et al*., 2009), as well as for cyclin E2 by ChIP assays. Our data strongly suggested that JDP2 was recruited to the promoters of genes for cyclin A2 and $p16^{Ink4a}$, but not for cyclin E2 (Figure 5C). However, we do not know the exact role of JDP2 in the modification of histone at and near the AP-1 site of the cyclin A2 promoter. The polycomb like transcriptional

repressor Bmi-1 causes the increases in levels of $p16^{Ink4a}$ and greatly reduces the self-renewal capacity of stem cells (Molofsky *et al*., 2003; Park *et al*., 2003). Sebastian *et al*. (2009) recently reported that overexpression of mixed-lineage leukemia 5 protein (MLL5; a trithorax homolog) indirectly regulates H3K4 methylation and represses expression of cyclin A2, with resultant promotion of myogenic differentiation. MLL5 indirectly represses the ability of both LSD1 and Set7/9 to methylate H3K4. Although we do not yet know the details of possible molecular interactions between JDP2 and the MLL complex on the cyclin A2 promoter, Nakade *et al.* (2009) reported the interaction of JDP2 with histone H3K27, which prevented methylation through the polycomb complexes PRC1 and PRC2. It is possible that JDP2 might bind to histone H3K4 for regulation of the gene for cyclin A2. Moreover, we previously reported that JDP2 can inhibit histone acetylation by p300, in particular the acetylation of H3, H4K8 and H4K16 residues *in vivo*, as well as the nucleosome-assembly activity (Jin *et al*., 2006). Mateo *et al*. (2009) also showed that the degradation of cyclin A is regulated by acetylation mediated by P/CAF. In fact, we found that JDP2 associated and colocalized with cyclin A in the nucleus by studies of cytochemistry (Supplementary Figure 6) and IP-Western blotting (data not shown). Therefore it is possible to JDP2 may regulate the stability of cyclin A2 through acetylation. Taken together, the repression of the expression of cyclin A2 is clearly due to the DNA-binding activity of JDP2 through AP-1 site. Not only binding to DNA but also INHAT by JDP2 or control of cyclin A stability by JDP2 (data not shown) might play a critical role in the negative regulation of expression of the gene for cyclin A2. The molecular interaction studies of the role of JDP2 in mediating acetylation by P/CAF and degradation of cyclin A2 are in progress in our laboratory.

In summary, our data indicate that JDP2 plays a role in suppression of the expression of cyclin A2, with subsequent inhibition of the kinase activity of cyclin A2-cdk2 and, finally, the suppression of cell proliferation. This hypothesis was supported by the results of overexpression of JDP2 encoded by a recombinant adenovirus and of gene-suppression experiments with siRNA (Figure 9). It is clear, moreover, that depletion of JDP2 interferes with progression of the cell cycle but not apoptosis.

Acknowledgements

We thank S. Itohara, C. Jin, R. Chiu, K. Itakura, T. Kondo, S. Takahashi, F. Kourilsky and G. Gachelin for comments on the original manuscript and M. Nakajima, K. Inabe, Y. Kusa and M. Hirose for their skilled technical assistance. This work was supported by grants from the RIKEN Bioresource Project (to K.K.Y.) and the Ministry of Education, Culture, Sport, Science and Technology of Japan (19041069 to K.K.Y.) and by a grant from Kaohsiung Medical University, Taiwan (KMU-EM-98-3).

References

Andrecht S, Kolbus A, Hartenstein B, Angel P, Schoropp-Kistner M. (2002). Cell cycle promoting activity of JunB through cylcin A activation. *J Bilol Chem* **277:** 35961-35968.

Aronheim A, Zandi, E., Hennemann, H., Elledge SJ, Karin M. (1997). Isolation of an AP-1 repressor by a novel method for detecting protein-protein interactions. *Mol Cell Biol* **17:** 3094-3102.

Bakiri I, Lallenmand D, Bossy-Wetzel E, Yaniv M. (2000). Cell cycle-dependent variations in c-Jun and JunB phosphorylation: a role in the control of cyclin D1

expression. *EMBO J* **19:** 2056-2068.

Blazek E, Wasmer S, Kruse U, Aronheim A, Aoki M, Vogt PK. (2003). Partial oncogenic transformation of chicken embryo fibroblasts by Jun dimerization protein 2, a negative regulator of TRE- and CRE-dependent transcription. *Oncogene* **22:** 2151-2159.

Broder YC, Katz S, Aronheim A. (1998). The ras recruitment system, a novel approach to the study of protein-protein interactions. *Curr Biol* **8:**1121-1124.

Casalino L, De Cesare D, Verde P. (2003). Accumulation of Fra-1 in ras-transformed cells depends on both transcriptional autoregulation and MEK-dependent poat-transciptional stabilization. *Mol Cell Biol* **23:** 4401-4415.

Casalino L, Bakiri L, Talotta F, Weitaman JB, Fusco A, Yaniv M *et al*. (2007). Fra-1 promotes growth and survival in RAS-transformed thyroid cells by controlling cyclin A transcription. *EMBO J* **26:** 1878-1890.

Chaudhry, HW, Dashoush, NH, Tang, H, Zhang L, Wang X, Wu, EX *et al*. (2004). Cyclin A2 mediates cardiomyocyte mitosis in the postmitotic myocardium. *J Biol Chem* **279:** 35858-35866.

Farras R, Bossis G, Andermarcher E, Jariel-Enconte I, Piechaczyk M. (2005). Mechanism of delivery of ubiquitylated protein to the proteasome: new target for anti-cancer therapy? *Crit Rev Oncol Hematol* 54: 31-51.

Farras R, Baldin V, Gallach S, Acquaviva C, Bossis G, Jariel-Encontre I *et al*. (2008). JunB breakdown in mid/lateG2 is required for down-regulation of cyclin A2 levels and proper mitosis. *Mol Cell Biol* **28:** 4173-4187.

Furono N, den Elzen N, Pines, J. (1999). Human cyclin A is required for mitosis until mid prophase. *J Cell Biol* **147;** 295-306.

Grana X, Reddy EP. (1995). Cell cycle control in mammalian cells: role of cyclins, cyclin dependent kinases (CDKs), growth suppressor genes and cyclin-dependent kinase inhibitors (CKIs). *Oncogene* **11:** 211-219.

Heinrich R, Levine E, Ban-Izhak O, Aronheim A. (2004). The c-jun dimerization protein 2 inhibits cell transformation and acts as a tumor suppressor gene. *J Biol Chem* **279:** 5708-5715.

Hwang HC, Matins CP, Bronkhorst Y, Randel E, Bern A, Fero M *et al*. (2002). Identification of oncogene collaborating with p27Kip1 loss by insertional mutagenesis and high-throughput insertion site analysis. *Proc Natl Acad Sci USA* **99:** 11293-11298.

Jin C, Ugai H, Song J, Murata T, Nili F, Sun K *et al*. (2001). Identification of mouse Jun dimerization protein 2 as a novel repressor of ATF-2. *FEBS Lett* **489:** 34-41.

Jin C, Li H, Murata T, Sun K, Horikoshi M, Chiu R et al. (2002). JDP2, a repressor of AP-1, recruits a histone deacetylase 3 complex to inhibit the retinoic acid-induced differentiation of F9 cells. *Mol Cell Biol* **22:** 4815-4826.

Jin C, Kato K, Chimura T, Yamasaki T, Nakade K, Murata T *et al*. (2006). Regulation of histone acetylation and nucleosome assembly by transcription factor JDP2. *Nat Struc Mol Biol* **13:** 331-338.

Kalaszczynska I, Geng Y, Iino T, Mizino S-I, Choi Y, Kondratiuk I *et al*. (2009). Cyclin A is redundant in fibroblasts but essential in hematopoietic and embryonic stem cells. *Cell* **138:** 1-14.

Kawaide R, Ohtsuka T, Okutsu J, Takahashi T, Kadono Y, Oda H *et al*. (2003) Jun dimerization protein 2 (JDP2), a member of the AP-1 family of transcription factors, mediates osteoclast differentiation induced by RANKL. *J Exp Med* **197:** 1029-1035.

Kramer A, Carstens CP, Wassermann WW, Fahl WE. (1997). CBP/cycA, a CCAAT-binding protein necessary for adhesion-dependent cyclin A transcription, consists of NF-Y and a novel Mr 115,000 subunit. *Cancer Res* **57:** 5117-5121.

Lerdrup M, Holmberg C, Dietrich N, Shaulian E, Herdegen T, Jaatela M *et al*. (2005). Depletion of the AP-1 repressor JDP2 induces cell death similar to apoptosis. *Biochim Biophys Acta* **1745:** 29-37.

Malumbres M, Barbacid M. (2009). Cell cycle, CDKs and cancer: a changing paradigm. *Nature Rev Cancer* **9:** 153-166.

Mateo F, Vidal-Laliena M, Canela N, Busino L, Martinez-Balbas MA, Pagano M *et al*. (2009). Degradation of cyclin A is regulated by acetylation. *Oncogene* **28:** 2654-2666.

Miyake S, Makimura M, Kanegae Y, Harada S, Sato Y, Takamori K *et al*. (1996). Efficient generation of recombinant adenoviruses using adenovirus DNA-terminal protein complex and a cosmid bearing the full-length virus genome. *Proc Natl Acad Sci USA* **93:** 1320-1324.

Molofsky AV, Pardal R, Iwashita T., Park IK, Clarka MF, Morrison SJ. (2003). Bmi-1dependence distinguishes neural stem cells self-renewal from progenitor proliferation. *Nature* **425:** 962-967

Mullany LK, Nelsen CJ, Hanse EA., Goggin MM, Anttila CK, Peterson M *et al*. (2007). Akt-mediated liver growth promotes induction of cyclin E through a novel translational mechanism and p21-mediated cell cycle arrest. *J Biol Chem* **282:** 21244-21252.

Nakade K, Pan J, Yoshiki A, Ugai H, Kimura M, Liu B *et al*. (2007). JDP2 suppresses adipocyte differentiation by regulating histone acetylation. *Cell Death Differ* **14:**

1398-1405.

Nakade K, Pan J, Yamasaki T, Murata T, Wasylyk B, Yokoyama KK. (2009). JDP2-(Jun Dimerization Protein 2)-deficient mouse embryonic fibroblasts are resistant to replicative senescence. *J Biol Chem* **284:** 10808-10817.

Ostrovsky O, Bengal E, Aronheim A. (2002). Induction of terminal differentiation by the c-jun dimerization protein 2 JDP2 in C2 myoblasts and rhabdomyosarcoma cells. *J Biol Chem* **277:** 40043-40054.

Pagano M, Pepperkok R, Verde F, Ansorge W, Draetta G. (1992). Cyclin A is required at two points in the human cell cycle. *EMBO J* **11:** 961-971.

Park IK, Qion D, Kiel M, Becker MW, Pihaija N, Weisman IL *et al*. (2003). Bmi-1 is required for maintenance of adult self- renewing hematopoietic stem cells. *Nature* **423:** 302-305.

Passegue E, Wagner EF. (2000). JunB suppresses cell proliferation by transcriptional activation of p16(Ink4a) expression. *EMBO J* **19:** 2969-2979.

Passegue E, Jochum W, Schorpp-Kirtner M, Mohle-Steinein U, Wagner EF. (2001). Chronic myeloid leukemia with increased granulocyte progenitors in mice lacking junB expression in the myeloid lineage. *Cell* **104:** 21-32.

Piechaczyk M, Farras R. (2008). Regulation and function of JunB in cell proliferation. *Biochem Soc Trans* **36:** 864-867.

Piu F, Aronheim A, Katz S, Karin M. (2001). AP-1 repressor protein JDP-2; inhibition of UV-mediated apoptosis through p53 down-regulation. *Mol Cell Biol* **21:** 3012-3024.

Sebastian S, Sreenivas P, Sambasivan R, Cheedipudi S, Kandalla P, Pavlath GK *et al*. (2009). MLL5, a trithorax homolog, indirectly regulates H3K4 methylation,

represses cyclin A2 expression, and promotes myogenic differentiation. *Proc Natl Acad Sci USA* **106:** 4719-4724.

Sherr CJ, Roberts JM. (1999). CDK inhibitors: positive and negative regulators of G1-phase progression. *Genes Dev* **13:** 1501-1512.

Steiner P, Philipp A, Lukas J, Godden-Kent D, Pagano M, Mittnacht S *et al*. (1995). Identification of a Myc-dependent step during the formation of active G_1 cyclin-cdk complexes. *EMBO J* **14:** 4814-4826.

Sweeney C, Nurphy M, Kubelka M, Ravnik SE, Hawkins CF, Wolgemuth DJ *et al*. (1996). A distinct cyclin A is expressed in germ cells in the mouse. *Development* **122:** 53-64.

Tybulewicz VL, Crawford CE, Jackson PK, Bronson RT, Mulligan RC, (1991). Neonatal lethality and lymphopenia in mice with a homozygous disruption of the *c-abl* proto-oncogene. *Cell* **65:** 1153-1163.

Ugai H, Yamasaki T, Hirose M, Inabe K, Kujime Y, Terashima M *et al*. (2005). Purification of infectious adenovirus in two hours by ultracentrifugation and tangential flow filtration. *Biochem Biophys Res Comm* **331:** 1053-1060.

Vousden KH, Prives C. (2009). Blinded by the light: the growing complexity of p53. *Cell* **137:** 413-431.

Figure legends

Figure 1 Proliferation of cells of WT and *Jdp2*KO mice during wound healing *in vivo* and scratch-wound healing *in vitro*. (A) Full-thickness excision wounds were made aseptically with a 4-mm biopsy punch on the skin of WT and *Jdp2*KO C57BL6 x 129 mice and images of each wound are shown on days 1, 3, 6 and 10 after injury. (B)

Wound areas were calculated on days 3, 6 and 9 after injury. Mean values from three experiments are shown with standard deviations. (C) Skin was wounded as in (A) and then mice were injected intraperitoneally with 20 μl/g body weight of BrdU-labeling reagent (Roche) on days 1, 3 and 6 after wounding. Mice were sacrified 2.5 h after injection. Sections were stained with hematoxylin-eosin and immunostained with the BrdU labeling and detection kit (Roche). (D) Skin wounds and surrounding areas were excised with an 8-mm biopsy punch at the indicated times after injury. Total RNA was analysed by semi-quantitative RT-PCR with appropriate primers, as indicated on the right. (E) MEFs from WT and *Jdp2*KO mice were grown in DMEM and started of serum for 36 h. Confluent monolayers were scratched, and incubated in DMEM plus 15% FCS for 12 h and then photographed.

Figure 2 Proliferative properties of MEFs from WT and *Jdp2*KO mice. (A) The expression of JDP2 mRNA in embryos and in MEFs from WT and *Jdp2*KO mice was analyzed by Northern blotting. The blot was re-probed for analysis of GPDH mRNA as a loading control. (B) The expression of JDP2 in MEFs from WT and *Jdp2*KO mice was examined by Western blotting. (C) and (D) Proliferation of MEFs from WT and *Jdp2*KO mice. MEFs were cultured in 10-cm dishes with DMEM plus 10%FCS for 3 days and then re-inoculated at the same density for ten passages. Cell numbers were determined at each passage (C). In (D), MEFs were starved in DMEM plus 0.1% FCS for 36 h and then re-plated in DMEM plus 15% FCS and cultured for 5 days. MEFs were counted. (E) MEFs from WT and *Jdp2*KO mice were plated in gelatin-coated dishes. Colonies (of more than 2 mm in diameter) were counted two weeks later.

Figure 3 Proliferation of MEFs from WT and *Jdp2*KO mice. (A) Serum-starved cells (5 x 10^5) were cultured in DMEM plus 15% FCS for 18 h, stained with PI and subjected to

FACS analysis to determine the percentage of cells in each phase of the cell cycle. (B) The percentage of MEFs in the S-phase was determined after re-stimulation in the 15% FCS at 4-h intervals, as in (A). (C) MEFs were cultured in chamber slides in DMEM with 15% FCS for 12h and then pulse-labeled with 10 mM of BrdU for 3 h. Labeled cells were detected by immunostaining with BrdU-specific antibodies. Scale bars represents 100 μm. (D) Percentages of MEFs that were stained with BrdU-specific antibodies. Means of results of three experiments are shown.

Figure 4 Gene expression in WT and *Jdp2*KO MEFs, as determined by Western blotting, microarray analysis and real-time PCR. (A)Western blots of cell cycle-related proteins in MEFs from WT and *Jdp2*KO mice. MEFs were synchronized by serum starvation for 48 h and then re-stimulated with 15% FCS. MEFs were harvested 8 h, 12 h and 16 h after the addition of serum and cell lysates were prepared. (B) Summary of the microarray data obtained with mRNA from WT and *Jdp2*KO MEFs. (C) Validation of hybridization intensities. The correction coefficient with respect to relative changes in mRNA levels in two assays was higher than 0.8, indicating that the microarray data are valid. (D) Analysis by quantitative PCR of the expression of representative genes using mRNA from WT MEFs (gray lanes) and *Jdp2*KO MEFs (Black lanes). MEFs were harvested after serum induction for 3 h and 18 h and then real-time PCR was performed with primer sets for the indicated genes, as described in the text. The level of each respective mRNA in non-stimulated WT MEF was taken as 100.

Figure 5 Kinetics of expression of cell cycle-related genes in WT and *Jdp2*KO MEFs. (A) Relative levels of expression of genes for cyclin A2, JDP2 and c-fos during cell cycling. Serum-starved MEFs from *Jdp2*KO (KO; black squares) and WT (black circles) mice were re-stimulated with serum for 24 h. The relative levels of respective

mRNAs, normalized by reference to GPDH mRNA, were compared at indicated times. (B) Western blots of products of cell cycle-related genes in lysates of MEFs from *Jdp2*KO and WT mice at the indicated times. GPDH was used as the control. (C) ChIP assays with JDP2-specific antibodies of lysates of *Jdp2*KO and WT MEFs with and without stimulation with serum. DNA fragments of genes for cyclin A2, $p16^{Ink4a}$ and cyclin E2 were detected by PCR with respective primers (Supplementary Table2).

Figure 6 JDP2 negatively regulates expression of the gene for cyclin A2. (A) Schematic representation of the promoter of the cyclin A2 gene (nt -944 to +157) fused with a gene for luciferase gene. The series of deletion mutants of cyclin A2-luciferase are described in the text. The AP-1-like motif, AP-1 motif and CRE are indicated by a white box, a gray box and a black box, respectively. Point mutations in each motif are also indicated. (B) Reporter activities of cyclin A2-reporter deletion constructs pA2-L, pA2-M and pA2–N. One μg of cyclin A2 promoter-luciferase reporter plasmid and 200 ng of pSV-luc were used for transfection of 5 x 10^4 *Jdp2*KO MEF. Six h after transfection, MEFs were washed, incubated for another 48 h and assayed. (C) Luciferase activities of the point mutants of the cyclin A2 promoter-luciferase constructs were determined as in (B). (D) The pSV-luc plasmid was used as the control for transfections in comparisons of *Renilla* luciferase activities of MEFs from *Jdp2*KO and WT mice.

Figure 7 EMSAs with nuclear extracts (NE) with MEFs from WT and *Jdp2*KO mice. (A) NE of *Jdp2*KO MEFs (indicated as K), WT MEFs (indicated as W) and bovine serum albumin (BSA; indicated as B) were incubated with probes corresponding to the CRE (lanes 1-3), AP1-like sequence (AP1L; lanes 4 and 5), the AP-1 point mutant (mAP1, lanes 6 and 7) and AP-1 (lanes 8-15) in the presence of 10 pmol of unlabeled mAP1 oligodeoxynucleotide (lane 12) or 0.1 pmol, 1 pmol and 10 pmol of unlabeled

AP-1 oligodeoxynucleotide as competitor. Positions of shifted bands (B1) and free DNA probes (Free) are indicated. (B) Supershifting EMSA using NE from serum-starved MEFs (FCS-) or 15% serum-induced MEFs (FCS+) and the DNA probe that corresponded to AP-1. NE from WT MEFs (W) and *Jdp2*KO MEFs (K) were incubated without (odd lanes) or with (even lanes) antibodies specific for JDP2. B2 indicates the super-shifted bands, N indicates nonspecifically shifted bands and X indicates aggregated DNA-protein complexes that remained in wells of the gel. B1 and Free indicate protein-DNA complexes and free DNA probes. (C) Competition and super-shifting assays using NE of WT MEFs and the CRE DNA probe. Reaction mixtures containing nuclear extracts from WT MEFs were prepared without (lane 1) and with 0.1 pmol, 1 pmol and 10 pmol of unlabeled (cold) CRE probe (lanes 2-4) and antibodies specific for JDP2, pJDP2, c-jun, JunB, JunD, c-Fos and ATF-2 (lanes 5 to 11), as indicated. B2 indicates super-shifted bands of antibody-DNA-protein complexes (B2). B1 and Free indicate DNA-protein complexes and un-bound CRE probe.

Figure 8 Enhanced cyclinA2-cdk2 activity in *Jdp2*KO MEFs. Cells were synchronized and stimulated with serum as described in the text. (A) Western blots (Wes) of cyclin A2 and actin in whole-cell lysates (left panel) and NE (right panel). (B) Levels of cdk2-associated cyclin A2. Whole-cell extracts from WT and *Jdp2*KO MEFs were immunoprecipitated (IP) with antibodies specific for cdk2 and then immunoprecipitates were subjected to SDS-PAGE (10% acrylamide) and blotted with antibodies against cyclin A2 (upper panel) and cdk2 (middle panel). Control Wes of whole-cell extracts with antibodies specific for β -actin is indicated (lower panel). (C) Induction of cyclin A2-cdk2 phosphorylation of histone H1. Immunoprecipitates containing the cyclin A2-cdk complex were isolated from whole-cell extracts (400 μg total protein) with cyclin

A2-specific antibodies and the histone H1-phosphorylating activity was determined *in vitro* as described in the text.

Figure 9 Effects of ectopic JDP2 and siRNA specific for JDP2 on proliferation and the expression of cyclin A2. (A) Reduced proliferation of WT and *Jdp2*KO MEFs upon expression of the JDP2 expression vector. 2 x 10^4 WT and *Jdp2*KO MEFs were transfected with 600 ng of pcDNA4-JDP2 or pcDNA and cells were counted three days later by the Alamar Blue method. The relative cell number on day 0 is given as 1. Means of results of three experiments ± SD are shown. (B) Depressed clyclin A2 reporter activity upon introduction of the JDP2 expression vector. We introduced 600 ng of pJDP2 or pcDNA4 and 400 ng of pA2M or pA2mAP1 into 5 x 10^4 *Jdp2*KO MEFs, incubated cells for 30 h and then measured luciferase activities. (C) Depressed proliferation of MEFs upon infection with Adeno-JDP2. 2 x 10^4 WT and *Jdp2*KO MEFs were infected with recombinant adenovirus Ad-JDP2 or β-galactosidase-encoding cDNA (Ad-cont) at an m.o.i of 1 and 10. Cells growth was counted five days later. (D) Depressed expression of mRNA for cyclin A2 in *Jdp2*KO MEFs infected with Ad-JDP2. The culture and infection of cells are described in the legend to (C). The expression of mRNA specific for cyclin A2 was quantitated by real-time PCR as described in the legend to Fig. 7A. (E) and (F) Effects of siRNA specific for JDP2 on proliferation and the expression of cyclin A2. WT MEFs (5 x 10^5 cells) were transfected with 30 pmole of siRNA specific for JDP2 (JDP2si#1 and #2)and non-specific double-stranded RNA (CONTsi). Three days transfection, cells were harvested and counted (E) and total RNA was subjected to real-time PCR with primers specific for JDP2 or cyclin A2 (F). Levels of expression were normalized by reference to that of

GPDH mRNA. Data are shown as percentages, relative to results for WT MEFs as a negative control.

Fig. 1

J. Pan *et al*.

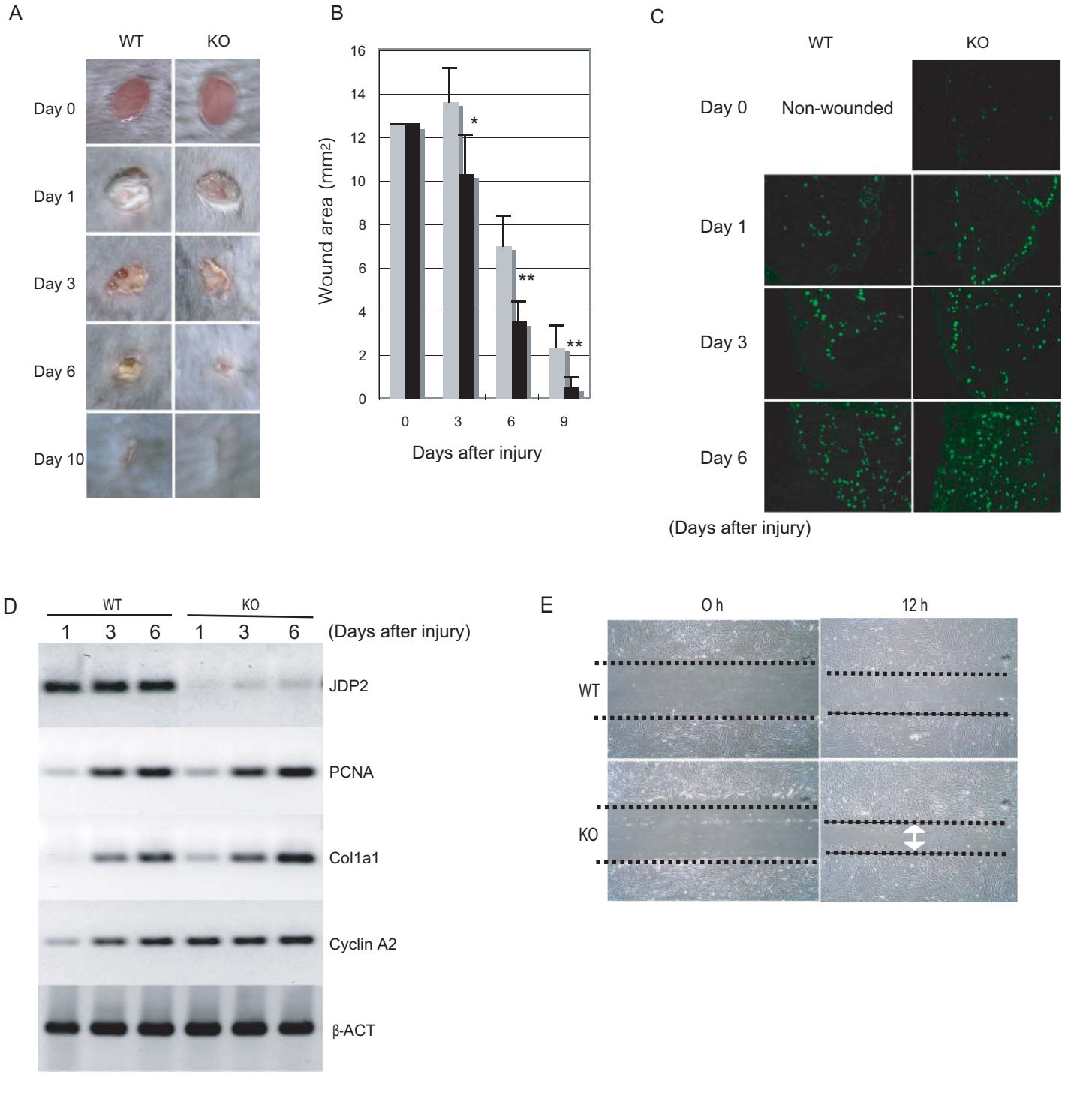

A

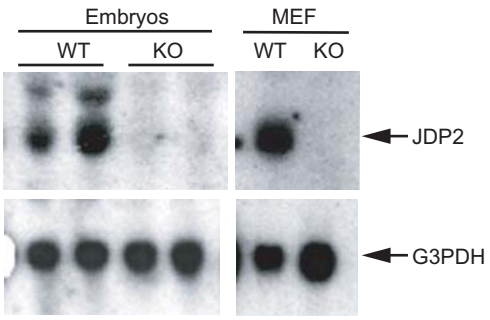
Embryos
MEF
WT
KO
WT
KO
JDP2
G3PDH

B

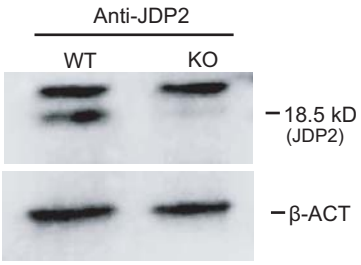
Anti-JDP2
WT
KO
18.5 kD
(JDP2)
β-ACT

C

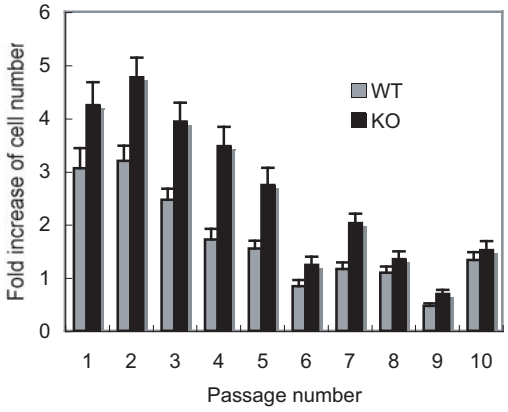
Fold increase of cell number
0
1
2
3
4
5
6
WT
KO
1
2
3
4
5
6
7
8
9
10
Passage number

D

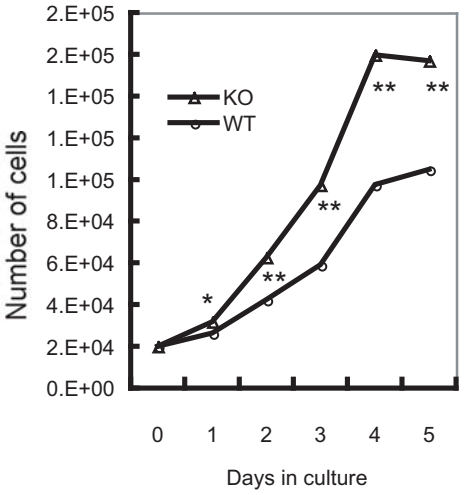
Number of cells
2.E+05
2.E+05
1.E+05
1.E+05
1.E+05
8.E+04
6.E+04
4.E+04
2.E+04
0.E+00
KO
WT
*
**
**
**
**
0
1
2
3
4
5
Days in culture

E

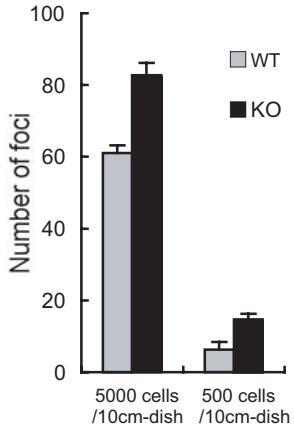
Number of foci
100
80
60
40
20
0
WT
KO
5000 cells
/10cm-dish
500 cells
/10cm-dish

Fig. 3

J. Pan *et al*.

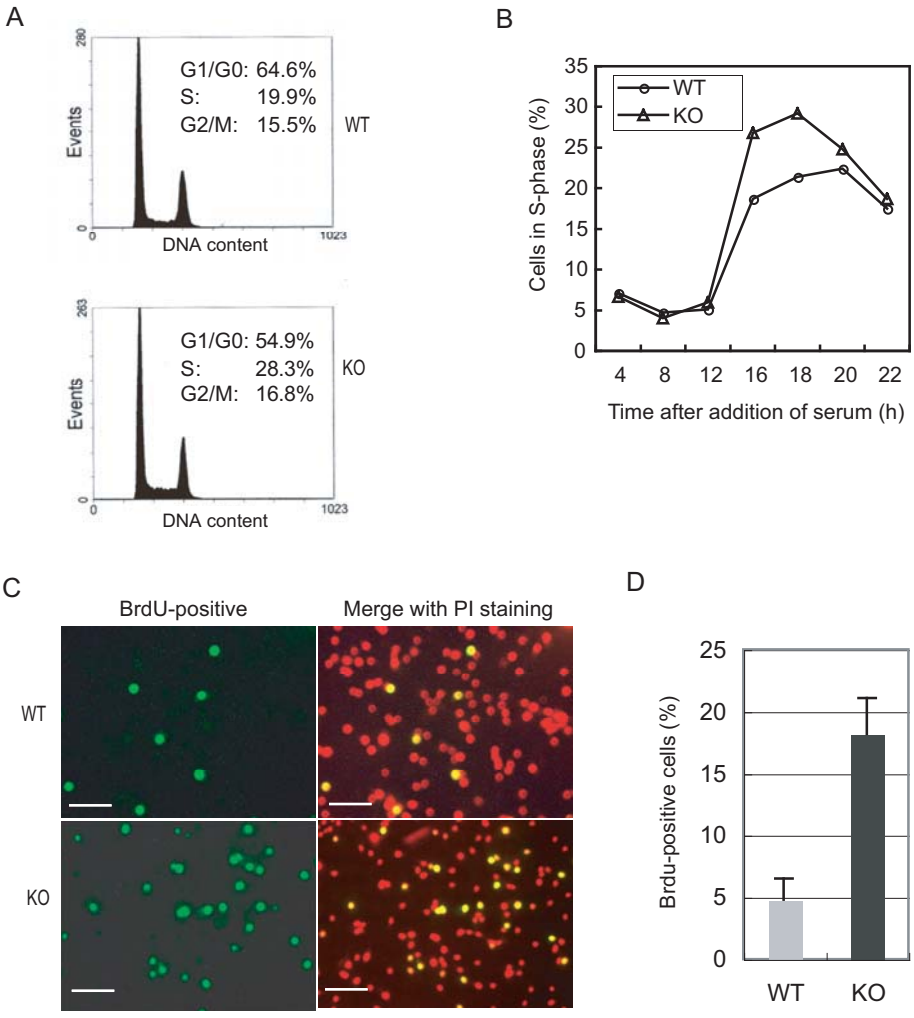

A

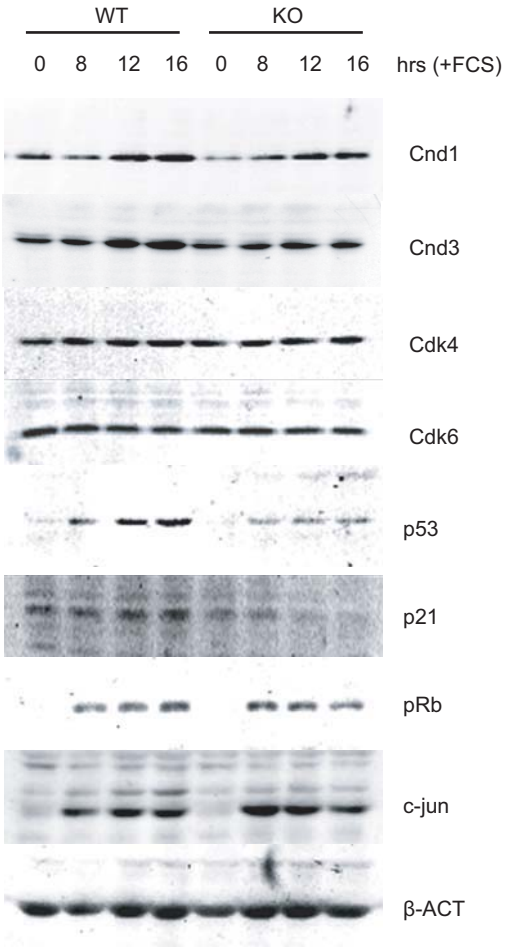

B

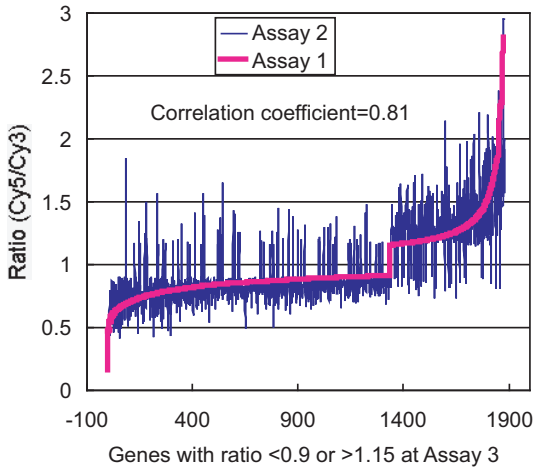

C

Symbol	Official gene name of gene product	KO / WT
Eif2s3y	Eukaryotic translation initiation factor 2, subunit 3	0.45
Hist1h2bc	Histone 1, H2bc	0.53
Fbln2	Fibulin 2	0.59
Ltbp1	Latent transforming growth factor beta-binding protein 1	1.80
Thbs4	Thrombospondin 4	2.27
Cxcl5	Chemokine (C-X-C motif) ligand 5	2.76
Cnd1	Cyclin D1	0.80
Cnc	Cyclin C	0.91
Cna1	Cyclin A1	0.96
Cnd3	Cyclin D3	0.98
Cne1	Cyclin E1	1.11
Cnb1	Cyclin B1	1.18
Cnb2	Cyclin B2	1.19
Cna2	Cyclin A2	1.32
Cne2	Cyclin E2	1.37
Cdkn2b	Cyclin-dependent kinase inhibitor 2B (p15, inhibits CDK4)	0.66
Cdkn2a	Cyclin-dependent kinase inhibitor 2A (P16)	0.72
Cdkn1a	Cyclin-dependent kinase inhibitor 1A (P21)	0.73
Cdkn1b	Cyclin-dependent kinase inhibitor 1B (P27)	1.00
Rb1	Retinoblastoma 1	0.96
Trp53	Transformation related protein 53	1.05
Rbl1	Retinoblastoma-like 1 (p107)	1.10

D

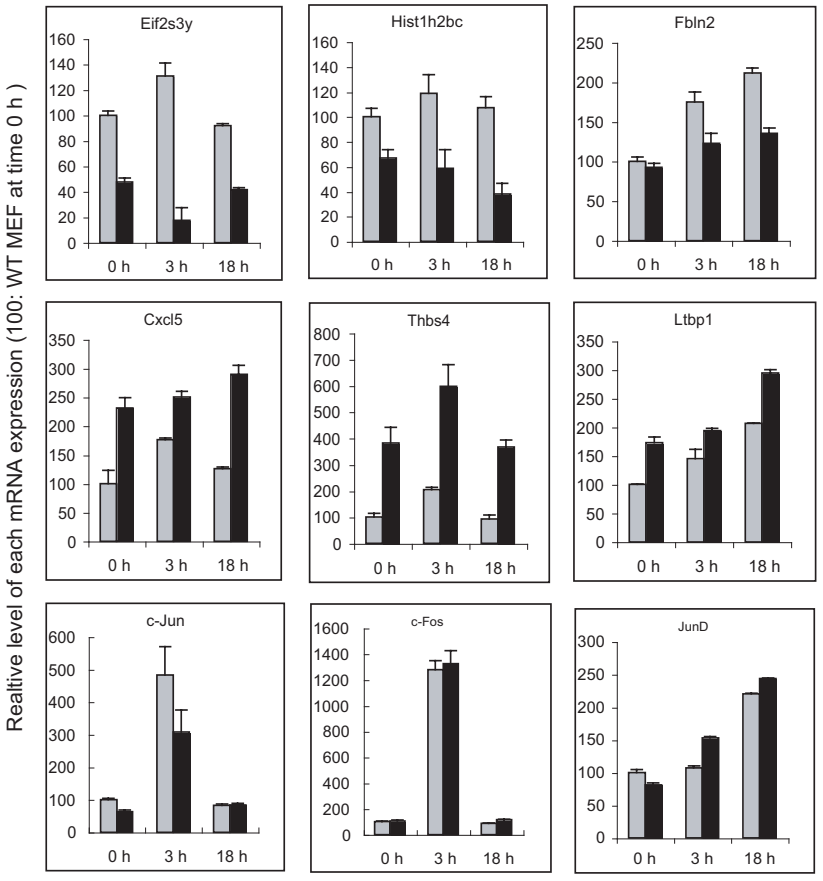

Fig. 5

J. Pan *et al*.

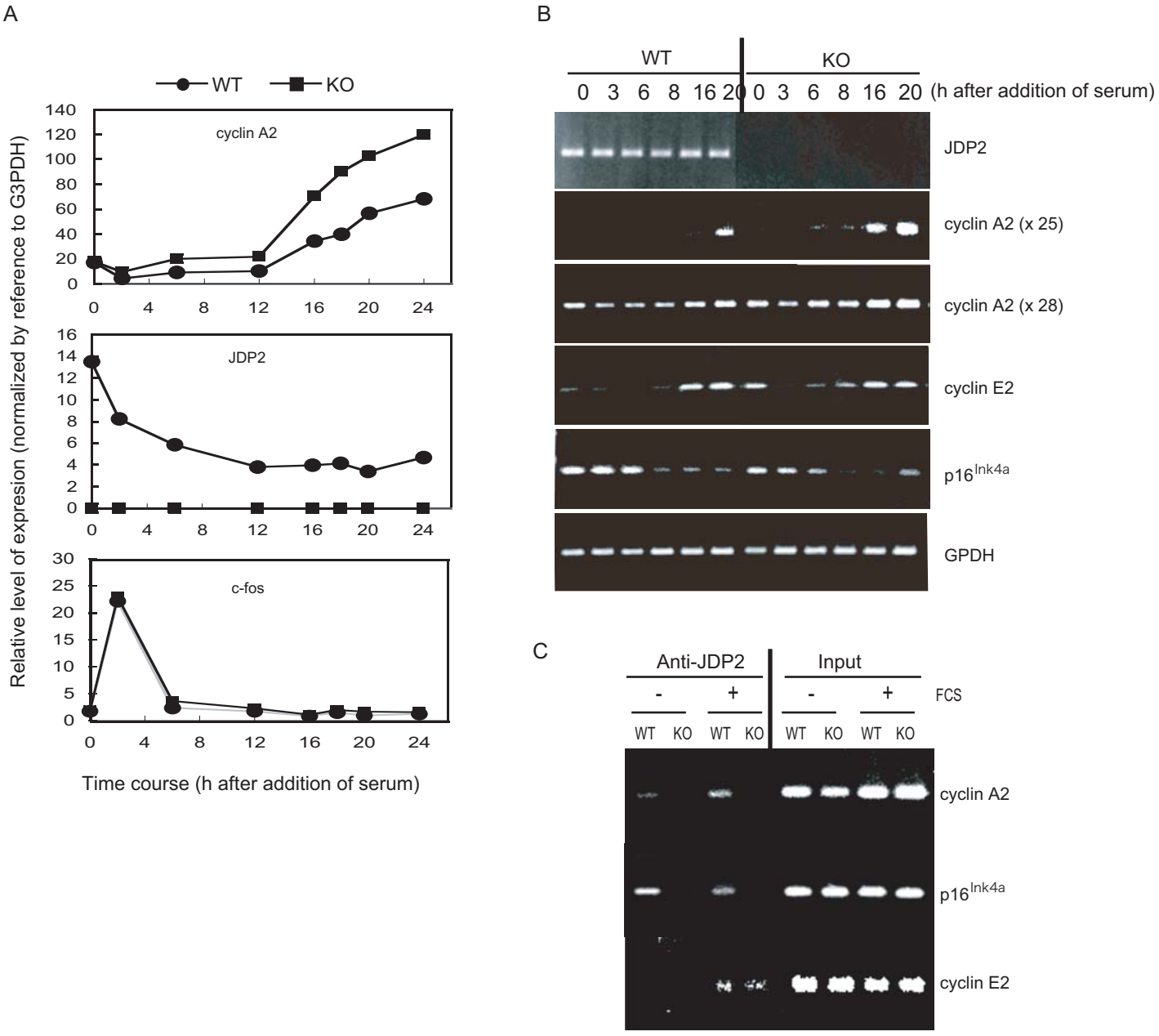

Fig. 6

J. Pan *et al*.

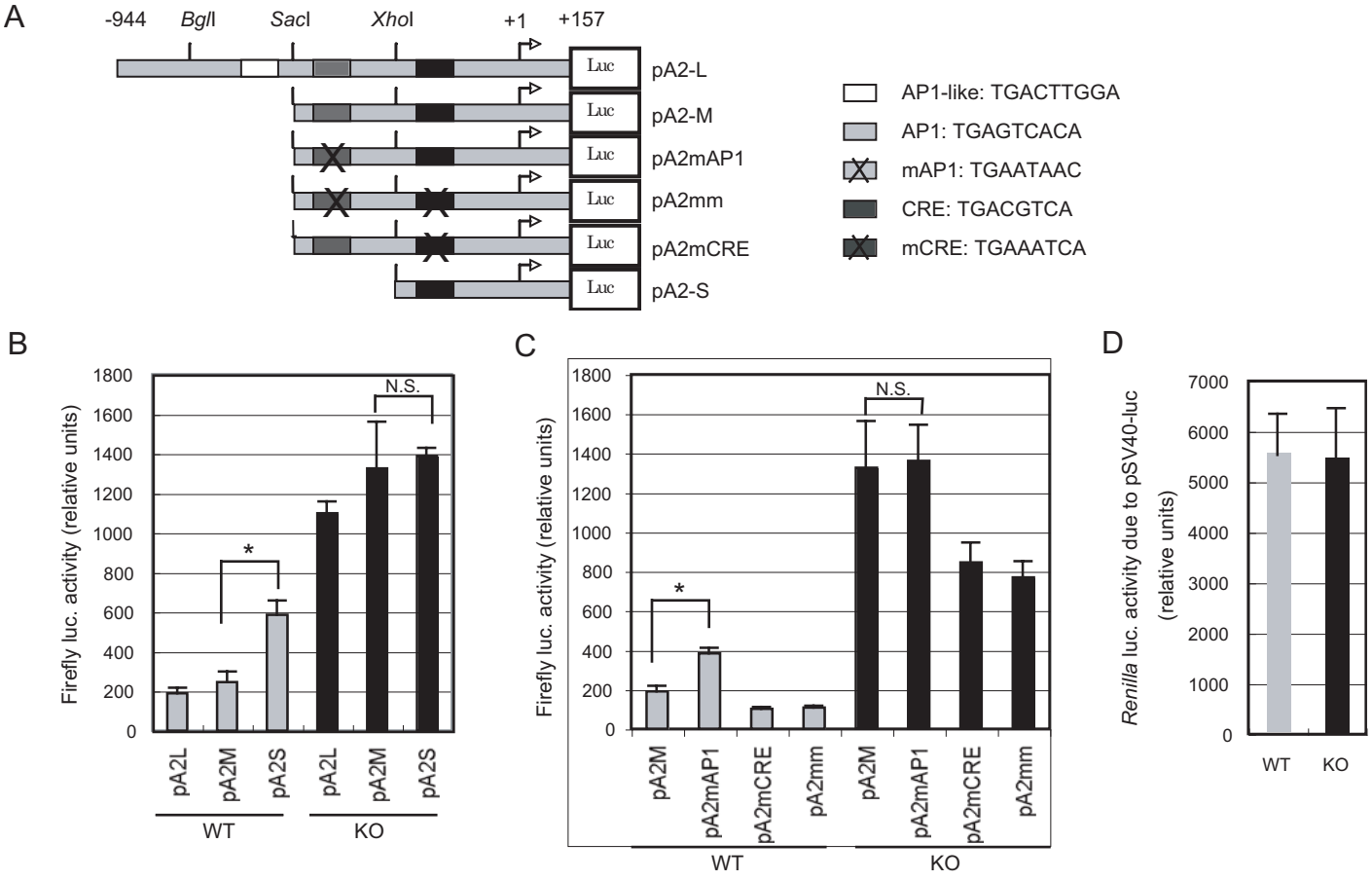

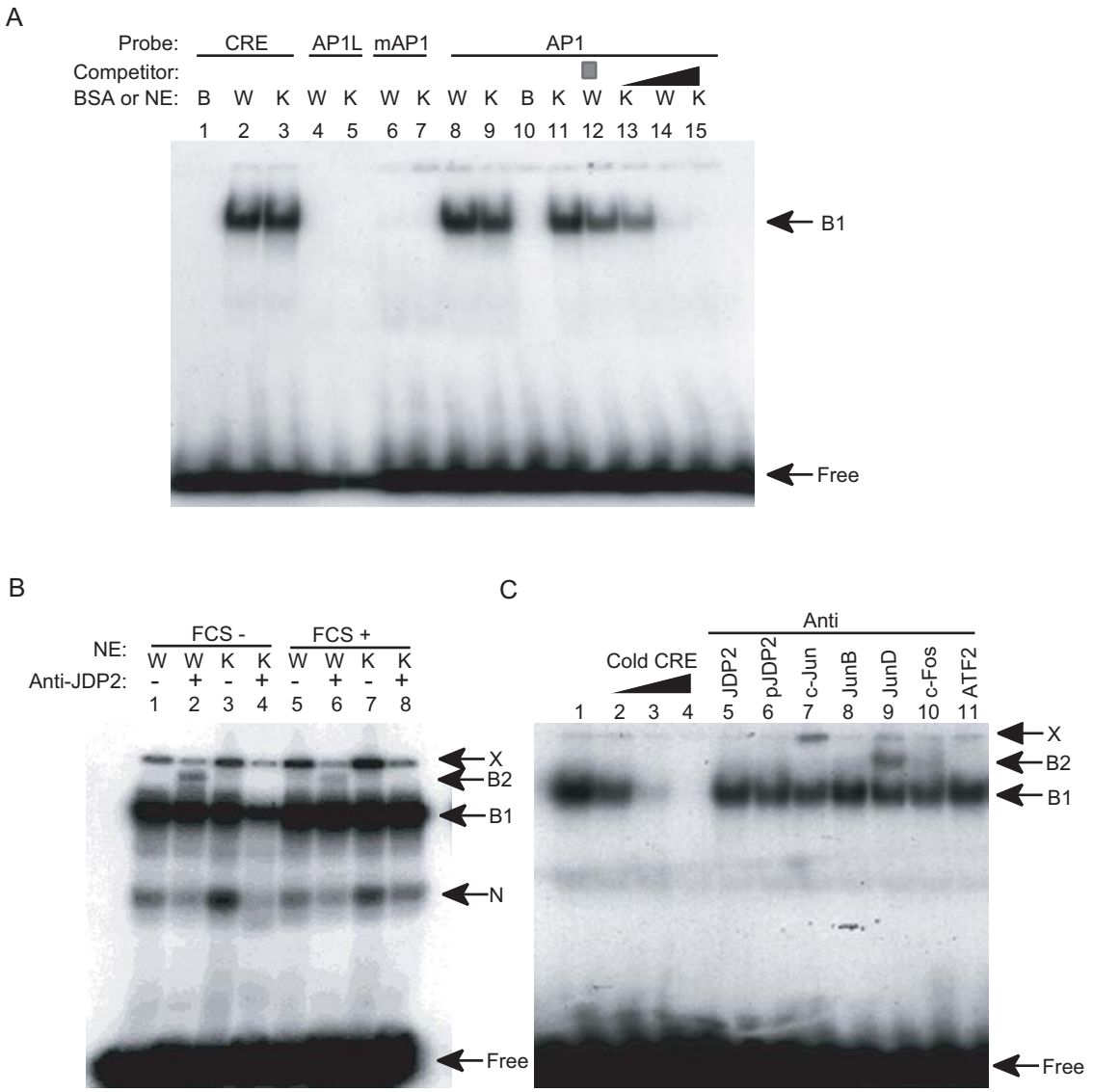
A
Probe: CRE AP1L mAP1 AP1
Competitor:
BSA or NE: B W K W K W K W K B K W K W K
1 2 3 4 5 6 7 8 9 10 11 12 13 14 15
B1
Free
B
NE: FCS - FCS +
W W K K W W K K
Anti-JDP2: - + - + - + - +
1 2 3 4 5 6 7 8
X
B2
B1
N
Free
C
Anti
Cold CRE
JDP2
pJDP2
c-Jun
JunB
JunD
c-Fos
ATF2
1 2 3 4 5 6 7 8 9 10 11
X
B2
B1
Free

Fig. 8

J. Pan *et al*.

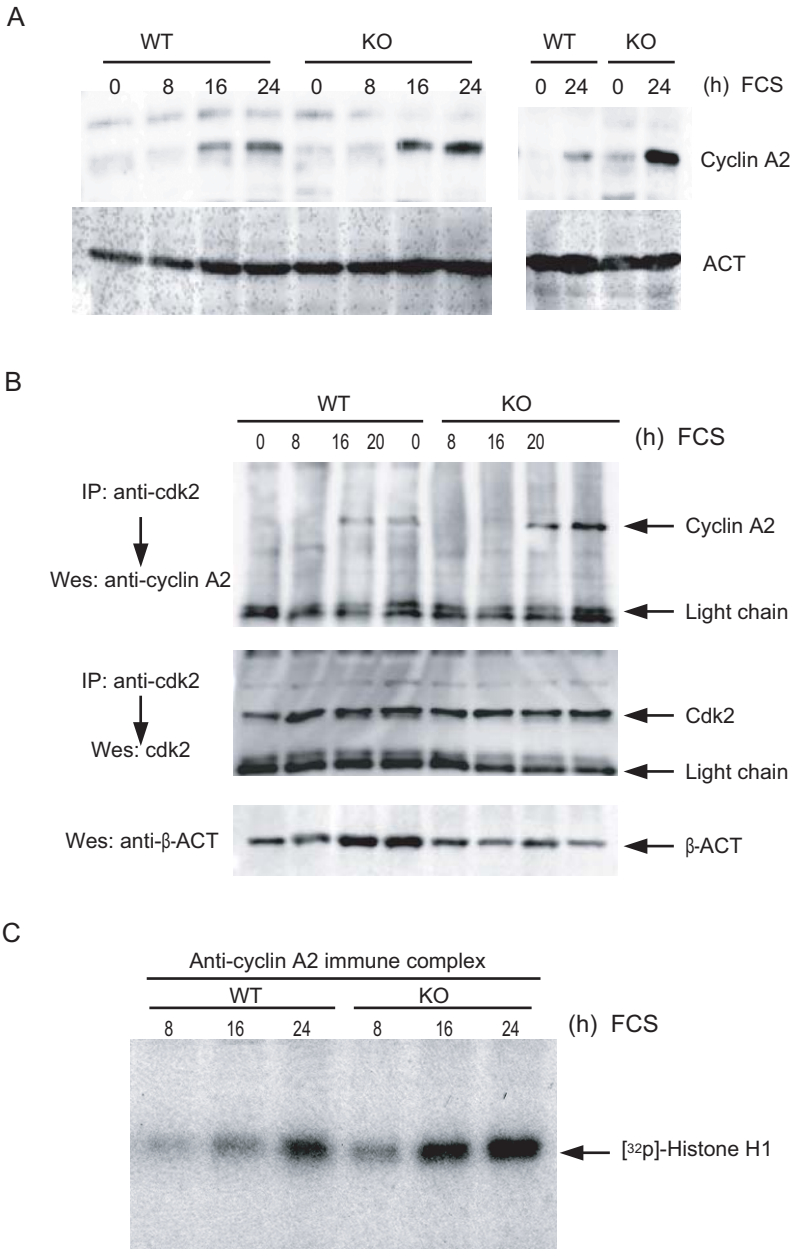

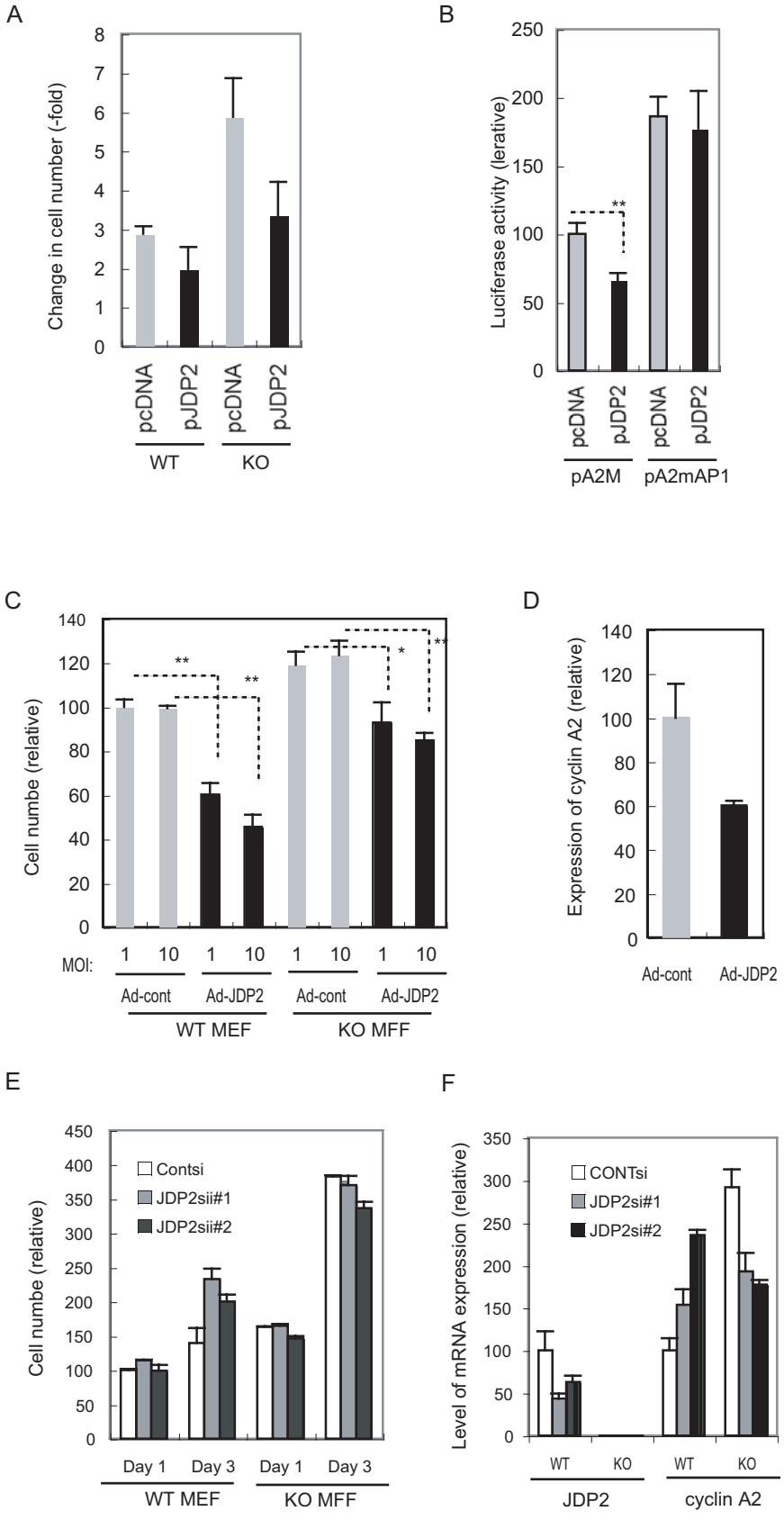
A
Change in cell number (-fold)
pcDNA
pJDP2
pcDNA
pJDP2
WT
KO
B
Luciferase activity (lerative)
**
pcDNA
pJDP2
pcDNA
pJDP2
pA2M
pA2mAP1
C
Cell numbe (relative)
**
**
*
**
MOI:
1
10
1
10
1
10
1
10
Ad-cont
Ad-JDP2
Ad-cont
Ad-JDP2
WT MEF
KO MFF
D
Expression of cyclin A2 (relative)
Ad-cont
Ad-JDP2
E
Cell numbe (relative)
Contsi
JDP2sii#1
JDP2sii#2
Day 1
Day 3
Day 1
Day 3
WT MEF
KO MFF
F
Level of mRNA expression (relative)
CONTsi
JDP2si#1
JDP2si#2
WT
KO
WT
KO
JDP2
cyclin A2